Kinetics Studies on a Multicomponent Knoevenagel–Michael Domino Reaction by an Automated Flow Reactor

Christian P. Haas and Ulrich Tallarek*[a]

The optimization of complex chemical reaction systems is often a troublesome and time-consuming process. The application of modern technologies, including automated reactors and analytics, opens the avenue for generating large data sets on chemical reaction processes in a short period of time. In this work, an automated flow reactor is used to present detailed kinetics and mechanistic studies about an amine-catalyzed Knoevenagel–Michael domino reaction to yield tetrahydrochromene derivatives. High-performance monoliths as catalyst supports and online coupled HPLC analysis allow for time-efficient data generation. We show that the two-step multicomponent domino reaction does not follow the kinetics of consecutive reaction steps proceeding independently from each other. Instead, the starting materials of both individual reactions compete for the active sites on the heterogeneous catalyst, which lowers the rate constants of both steps. This knowledge was used to implement a more efficient experimental setup which increased the turnover numbers of the catalyst, without adjusting common reaction parameters like temperature, reaction time, and concentrations.

Introduction

Catalysis was recently described as the science and technology of influencing the rates of chemical reactions.[1] Thereby, "influencing" usually means, just like with uncatalyzed reactions, aiming at optimization, i.e., maximization, of the desired reaction rates (while suppressing side reactions) to achieve maximum conversion, productivity, and selectivity. This optimization is still predominantly performed by the experimentalist in labor-intensive batch reactions, typically allowing only a few experiments per day.[2] Thanks to the rapid technological change combined with a much stronger interplay between chemical synthesis and the engineering disciplines, this drawback was recently overcome, as documented by reports on, e.g., self-optimizing automated flow reactors,[3] algorithm-based optimum catalyst selection,[4] or the discovery of new reactivities by an organic synthesis robot using machine learning.[5] Importantly, all these studies utilize platforms that fully-automatically collect a large amount of data in a short period of time with the general ambition to transform synthetic chemistry into a more data-driven discipline.[6,7]

We have recently presented an automated flow system that relies on an efficient combination of a continuous-flow microreactor and an online coupled HPLC analysis system to rapidly collect data on heterogeneous catalytic reactions.[8,9] However, we did not focus on optimization, but on investigating the selected reaction process in detail to derive mechanistic conclusions from the reaction kinetics (rate constants, reaction orders, and activation energies) and to characterize the catalyst support (e.g., transport versus reaction limitations, catalyst effectiveness). Based on our previous reports, this work presents a follow-up study where the derived kinetic information is directly implemented into process optimization. Most relevant aspects regarding the functionality of the microreactor are briefly summarized below.

To address the intrinsic kinetics of a heterogeneous catalytic reaction, we introduced benchmarked, commercially available, hierarchical (macro–mesoporous) silica-based monoliths as high-performance catalyst supports.[8–10] Their use allows to shift the solid–liquid operation from diffusion-limited to reaction-controlled conditions by combining unhindered access to a large mesopore surface area ($\sim 250\ m^2\,g^{-1}$) inside the monolith skeleton with hydrodynamic plug-flow behavior in the macropore space of the microreactor. Although mesopore space and macropore space are microscopically disordered, their three-dimensional physical reconstruction combined with morphological analysis as well as fluid flow and mass transport simulations yielded quantitative morphology–transport relationships for these materials.[11–14] A summary of relevant morphological features of silica monoliths, which are also employed in the present work, and useful further background information can be found in Section S1 and Figure S1 of the Supporting Information (SI).

Through these unique morphological features the monolith-supported microreactor preserves its plug-flow characteristic over a wide range of liquid flow rates.[8] Therefore, a comprehensive set of reaction times can be realized in a single

[a] C. P. Haas, Prof. U. Tallarek
Department of Chemistry
Philipps-Universität Marburg
Hans-Meerwein-Strasse 4, D-35032 Marburg (Germany)
E-mail: tallarek@staff.uni-marburg.de

flow experiment just by variation of the volumetric flow rate, itself precisely controlled by the pumping unit. These conditions form the basis for a high-resolution reaction time control.[15–17]

In this work, the described combination of a plug-flow catalytic microreactor and an automated flow system allows us to resolve in a fast and convenient manner the kinetics of a primary-amine catalyzed Knoevenagel–Michael domino reaction to tetrahydrochromene derivatives (Scheme 1). The importance of multicomponent domino reactions, in general, as well as of the chosen reaction system, in particular, have been broadly covered over the years and in recent reports,[18–23] so that we will not discuss further details here. However, even with a wide variety of catalysts and a large number of proposed reaction mechanisms reported, a systematic investigation on how a catalyst is capable of catalyzing simultaneously two different reactions is missing. With this work, we close this gap by recording first the detailed kinetics of the individual reaction steps and then implement the screened information in an optimized experimental design to perform the multicomponent reaction more efficiently regarding turnover frequencies of the catalytically active sites. To the best of our knowledge, this represents the first detailed kinetics study on a multicomponent one-pot synthesis in a flow reactor.

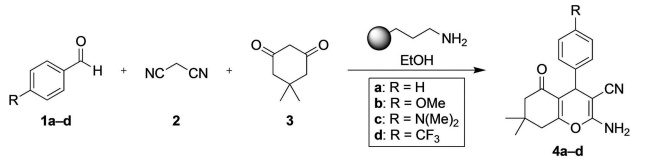

Scheme 1. Multicomponent domino reaction of aromatic aldehydes **1a–d**, malononitrile (**2**), and dimedone (**3**) to yield tetrahydrochromene derivatives **4a–d**. The reaction is heterogeneously base-catalyzed by aminopropylated silica and is conducted in the green solvent ethanol.

Results and Discussion

General Experimentation and Methodologies

General methodologies and applications of flow chemistry combined with heterogeneous catalysis are addressed in a variety of recent reviews, covering aspects from materials science and microreactor types to process safety and intensification.[24–30] Based on these principles, advanced techniques for continuous-flow kinetics studies were introduced, which use transient flow or temperature profiles to investigate the kinetics of chemical reactions.[31–34] Thereby, the reaction progress was investigated on microreactors operating under non-steady-state conditions in order to eliminate the time necessary to reach steady-state operation and, consequently, to reduce the amount of consumed starting material, experiment time, and produced waste.

In this work, we rely on steady-state operation, which allows us to directly correlate analytical results to starting concentrations and reaction times without additional assumptions or calculations. Reaction kinetics can be fitted directly to the recorded data. The increased amount of resources, however, is minimized by the small size of the high-performance catalyst support reducing reaction times on the microreactor. The flow system was equipped with an aminopropylated silica monolith of the type described above (4.6 mm inner diameter and 5 mm bed length). Despite a reactor void volume of only ~0.07 ml (taking a total porosity of ~0.86 for this monolithic material into account, cf. Section S1), this small reactor exhibits an available active surface area of ~6 m^2 to achieve quantifiable conversions in short reaction times (~4–21 s), while preserving the described high-resolution reaction time control.

The flow system was assembled from commercially available HPLC instrumentation (Figure S2 in the SI) and programmed to fully automatically adjust and control flow rates, mixing proportions, temperatures, as well as the timing of the online analytics. The flow chart for the automated flow reactor is shown in Figure S3. The continuous-flow reaction system was online coupled to an HPLC system through an injection valve (Figure S2). The chromatographic separation conditions in the HPLC domain were adjusted such that the samples could be analyzed quickly (in 2.5–5 min), with substrates, intermediates, and products always baseline-separated. Reaction input parameters like flow rate and substrate concentrations were changed after the injection into the HPLC dimension. The analysis time in the HPLC domain was sufficient to re-establish steady-state conditions on the microreactor (as controlled by an inline diode array detector (DAD), cf. Figure S3), prior to the next injection. Full experimental details are described in the Experimental Section and in the SI. Graphical illustrations of all programmed input variables, the controlled process parameters, as well as the resulting HPLC chromatograms for every conducted experiment are also presented in the SI.

Knoevenagel Condensation, Michael Addition, and Multicomponent Reaction Mechanism

Multicomponent domino reactions are predominantly reported in classical one-pot designs, where all substrates are added to the reactor at the same time. In the following, we will refer to the phrase "one-pot" for exactly this classical experiment design but are aware of the broader scope of one-pot syntheses.[35] In general, the success of multicomponent domino reactions in one-pot syntheses is based on the discrimination of distinct reaction rates. This means that the desired reaction rates are much higher than those behind undesired reactions, so that multiple consecutive reaction steps proceed without side reactions becoming important and selectivities approach unity. To investigate this principle in the kinetics data, the domino reaction was divided into its elementary reactions to allow the comparison of the individual reactions with the multicomponent one-pot operation. The chosen reaction process (Scheme 1) is discussed in detail only for one aldehyde, the

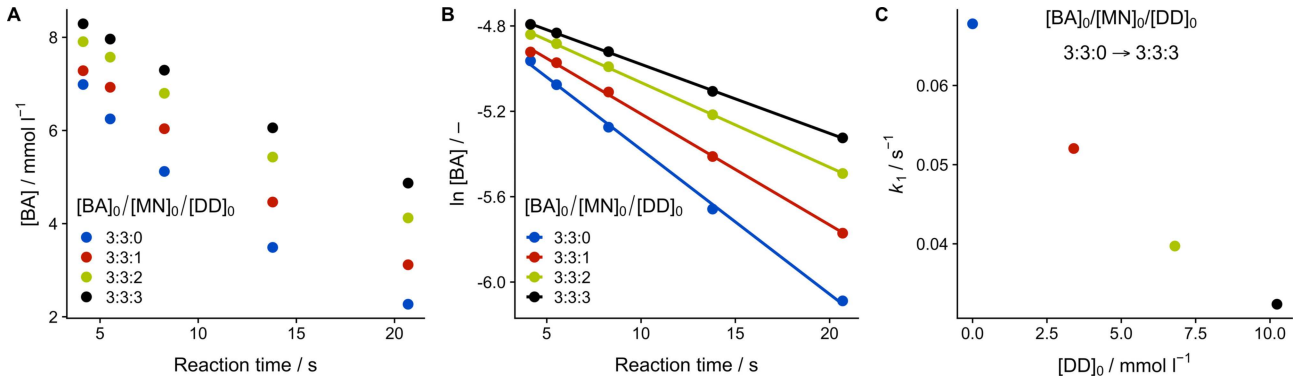

Figure 1. Experimental results for the Knoevenagel condensation with increasing dimedone starting concentration at 40 °C in ethanol. **A** Benzaldehyde concentration [BA] in the reaction solution as a function of the reaction time. **B** Logarithmic benzaldehyde concentration versus reaction time, corresponding to a first-order reaction kinetics (equation 2). **C** Obtained rate constants k_1 for the Knoevenagel condensation as a function of the dimedone starting concentration $[DD]_0$.

unsubstituted benzaldehyde (**1 a**) yielding the tetrahydrochromene derivative **4 a**. As we show later, the kinetics principles, which we observe for this particular reaction, can also be transferred to the substituted aromatic aldehydes **1 b**–**1 d**.

Starting with the Knoevenagel condensation as first elementary reaction, its reaction order was found by a variation of the starting concentrations of benzaldehyde $[BA]_0$ and malononitrile $[MN]_0$ on the reactor and comparing the reaction rates. Thereby, the overall order of the Knoevenagel reaction was determined as unity with respect to the benzaldehyde concentration [BA], resulting in the following differential (equation 1) and integrated (equation 2) rate laws:

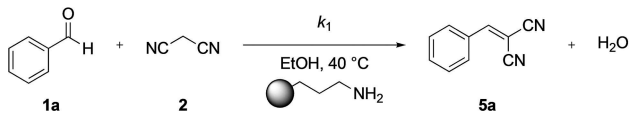

Scheme 2. Knoevenagel condensation of benzaldehyde (**1 a**) and malononitrile (**2**) to benzylidenemalononitrile (**5 a**) catalyzed by an aminopropylated silica monolith.

$$\frac{d[BA]}{dt} = -k_1 \cdot [BA] \quad (1)$$

$$[BA] = [BA]_0 \cdot e^{-k_1 t} \quad (2)$$

Here, k_1 represents the rate constant of the Knoevenagel condensation and t denotes the reaction time. The first-order reaction kinetics of this bimolecular reaction is explained by the well-known reaction mechanism of the primary-amine catalyzed Knoevenagel condensation between aromatic aldehydes and CH-acidic compounds.[8,36,37] The two-step mechanism starts with the condensation reaction of benzaldehyde (**1 a**) and the amine to yield an immobilized benzaldimine species. This first step appears to be the rate-determining step of the overall Knoevenagel condensation under the chosen reaction conditions. In the second step, a nucleophilic attack of the activated methylene group of malononitrile (**2**) on the benzaldimine species yields the Knoevenagel product benzylidenemalononitrile (**5 a**) (Scheme 2).

In the next step, the automated flow reactor screened different reaction times by adjusting the flow rate, first with Knoevenagel substrates **1 a** and **2** only and then with a stepwise increasing dimedone (**3**) starting concentration $[DD]_0$, to finally achieve the classical multicomponent reaction style in a one-pot design (equivalent ratios of $[BA]_0/[MN]_0/[DD]_0$ from 3:3:0 to 3:3:3, with 3 eq corresponding to a starting concentration of 10 mmol l^{-1}). In only 50 min experiment time, five reaction times for each of the four different compositions could be investigated and the resulting 20 chromatograms were analyzed by using previously performed calibration. With this information, the concentrations of the UV-Vis active benzaldehyde (**1 a**) and benzylidenemalononitrile (**5 a**) were plotted against reaction time and the kinetic model (equation 2) was fitted to the data to receive the rate constants k_1. As illustrated in Figure 1, the rate constants of the Knoevenagel condensation were strongly affected by the dimedone starting concentration $[DD]_0$, i.e., the k_1-values are reduced by more than half from the exclusive Knoevenagel reaction to the multicomponent reaction with equated equivalents. Therefore, dimedone appears to disturb the rate-determining first step of the Knoevenagel condensation, where benzaldehyde reacts with a primary amine to yield the benzaldimine intermediate. To understand the effect of dimedone on the active sites on the surface of the silica monolith, the kinetics of the Michael addition were recorded next.

The Michael reaction was run with the same protocol as applied for the Knoevenagel condensation, using commercially available benzylidenemalononitrile (**5 a**) and dimedone (**3**) to give the tetrahydrochromene derivative **4 a** (Scheme 3). In the first step, the reaction order was identified to follow a second-order kinetics with respect to the concentrations of benzylidenemalononitrile [BMN] and dimedone [DD] (equation 3). In contrast to the Knoevenagel condensation, both substrate

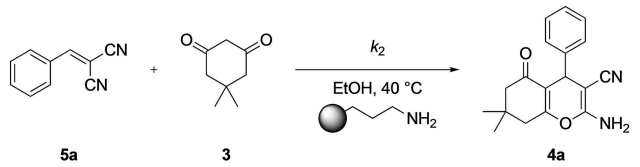

Scheme 3. Michael addition of dimedone (**3**) and benzylidenemalononitrile (**5 a**) with subsequent cyclization and tautomerization to yield the tetrahydrochromene derivative **4 a**, catalyzed by an aminopropylated silica monolith.

molecules are included in the rate law, indicating that the Michael addition of dimedone to benzylidenemalononitrile is rate determining. The reaction is proposed to follow an ion-pair mechanism, where dimedone ($pK_a \sim 5$) and the amine ($pK_b \sim 3.5$ for propylamine) first build an ion-pair through acid-base reaction.[38] The deprotonated dimedone then adds to the Knoevenagel product **5 a**, and after subsequent protonation, cyclization, and tautomerization, the final product of the domino reaction **4 a** is obtained. To fit the data for the rate constants k_2 of the Michael addition, the integrated rate law (equation 4) could be simplified due to equal starting concentrations of the substrates ($[BMN]_0 = [DD]_0 = 10\ mmol\ l^{-1}$):

$$\frac{d[BMN]}{dt} = \frac{d[DD]}{dt} = -k_2 \cdot [BMN] \cdot [DD] \quad (3)$$

$$\frac{1}{[BMN]} = \frac{1}{[DD]} = k_2 \cdot t + \frac{1}{[BMN]_0} \quad (4)$$

After fitting of the data according to equation 4 (Figure S4), rate constants k_2 were obtained for the exclusive Michael addition and for compositions with increasing benzaldehyde or malononitrile starting concentrations, $[BA]_0$ or $[MN]_0$, respectively. In the following, we begin with the impact of benzaldehyde on the Michael addition step.

As illustrated in Figure 2A, adding benzaldehyde to the ongoing Michael addition has a similar effect as adding dimedone to the Knoevenagel condensation – the rate constants k_2 are reduced by more than half from the exclusive Michael addition to conditions with equated equivalents of $[BA]_0$ and $[DD]_0$. Consequently, a competition must exist between these two substrates; one substrate blocks the active sites for reaction of the other. This "blockage" of the active sites should be reversible, since otherwise we would not expect any conversion in the one-pot reaction. Under steady-state operation of the microreactor, these reversible processes are completely equilibrated. We therefore propose a mechanism in accordance with mechanisms reported previously, but we add two crucial equilibria instead of irreversible reactions (Scheme 4): While an aminopropyl group on the reactor surface is occupied by a benzaldehyde molecule (in the form of a quasi-immobilized benzaldimine structure), the active site is in turn incapable of deprotonating dimedone molecules to generate the required ion-pairs for the nucleophilic attack in the Michael addition. Or put the other way around, the ammonium enolate ion-pair between the protonated aminopropyl group and the deprotonated dimedone does not allow benzaldehyde molecules to generate the required benzaldimine species, so that the active sites are blocked for the Knoevenagel condensation. Thus, competition between the substrates for the active sites in the multicomponent one-pot design reduces significantly the efficiency of the two individual reactions.

The question may arise if this finding plays a role for the multicomponent one-pot synthesis at all, since both reactions take place simultaneously on the reactor and both catalytically active forms of the catalyst coexist. The answer definitely is a "yes" for at least one part of the reactor, the region directly behind the reactor inlet. As long as the Knoevenagel product benzylidenemalononitrile (**5 a**) has not been produced on the reactor, dimedone (**3**) only hinders its production without the possibility to react itself. This issue is investigated further below, where we implement a flow setup consisting of a main reactor and a preceding smaller reactor exclusively for the Knoevenagel condensation, serving as initiator for the multicomponent reaction on the main reactor.

Figure 2B illustrates another observation in the Michael system with the added benzaldehyde (for $[BMN]_0/[DD]_0/[BA]_0 =$

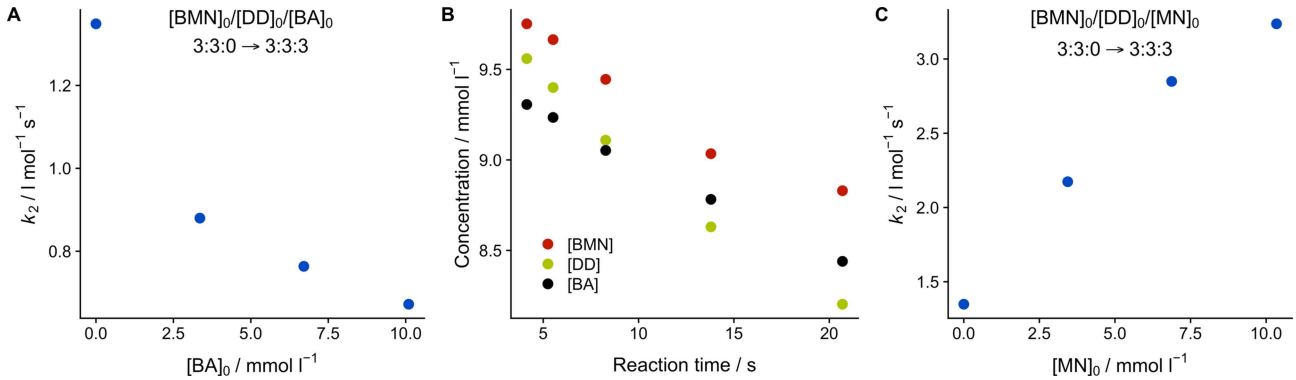

Figure 2. Experimental results for the Michael addition step with increasing concentrations of benzaldehyde and malononitrile at 40 °C in ethanol. **A** Obtained rate constants k_2 corresponding to a second-order kinetics (equation 4) as a function of the benzaldehyde starting concentration $[BA]_0$. **B** Concentrations of benzylidenemalononitrile [BMN], dimedone [DD], and benzaldehyde [BA] in the reaction solution as a function of the reaction time (for $[BMN]_0/[DD]_0/[BA]_0 = 3:3:3$), indicating the formation of side product. **C** Rate constants k_2 for the Michael addition versus malononitrile starting concentration $[MN]_0$.

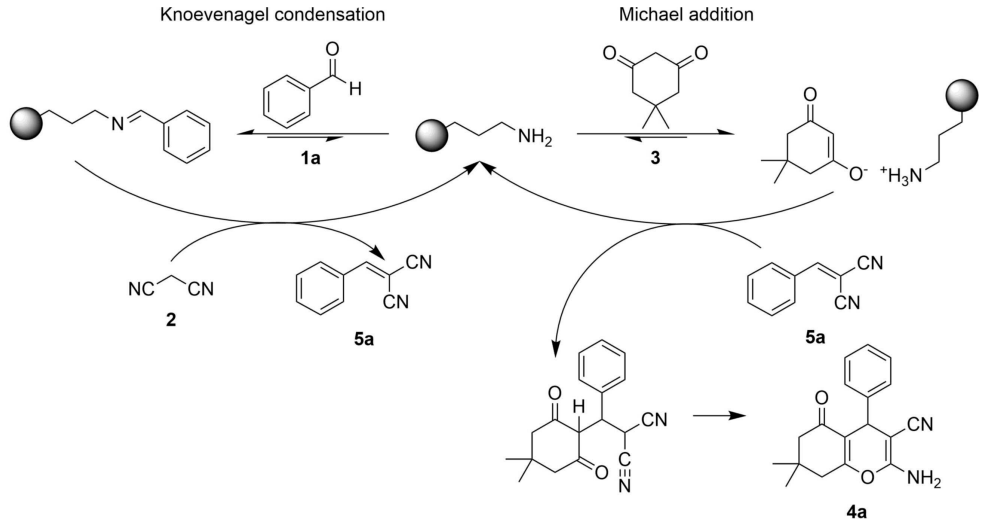

Scheme 4. Proposed reaction mechanism for the multicomponent domino reaction between benzaldehyde (**1a**), malononitrile (**2**), and dimedone (**3**) catalyzed by aminopropylated silica to yield the tetrahydrochromene derivative **4a**. The Knoevenagel condensation follows the primary-amine mechanism with benzaldimine intermediate, while the Michael addition follows the ion-pair mechanism, where dimedone is deprotonated prior to its nucleophilic attack on the Knoevenagel product **5a**. This results in competition for the active sites between both reactions.

3:3:3): The concentration of benzaldehyde decreases significantly over the reaction time. Moreover, the dimedone concentration seems to drop faster than that of benzylidenemalononitrile – although quantification of dimedone by UV-Vis must be treated cautiously due to its sensitive absorption, known to depend on the keto-enol ratio. However, this observation is readily explained by the Knoevenagel reaction between benzaldehyde and dimedone. With a significant rate constant, experimentally determined as 0.006 s^{-1} (Figure S5B) compared to $k_1 = 0.03\ s^{-1}$ for the malononitrile Knoevenagel condensation under multicomponent conditions, the one-pot synthesis should also generate a significant amount of side product. Yet, nothing in this regard could be observed and the multicomponent reactions proceeded with highest selectivities (~1). For a plausible explanation, the state of the active sites should be considered. With the Michael addition performed here (benzaldehyde added and malononitrile absent), the quasi-immobilized benzaldimine species can be enriched on the active reactor surface, because malononitrile is missing for the very fast second step of the Knoevenagel reaction. By contrast, under classical multicomponent conditions, the catalyst should be predominantly in its amine form and the rate constant of the dimedone-benzaldehyde Knoevenagel condensation should be much lower when malononitrile is present. This finally allows for the required discrimination of reaction rates in the one-pot domino reaction.

Moreover, we found the quite surprising result that malononitrile has an impact on the performance of the Michael addition, as illustrated by Figure 2C. The k_2-values of the reaction are increased by a factor of 2.4 when comparing the exclusive Michael addition ($[BMN]_0/[DD]_0/[MN]_0 = 3:3:0$) with conditions of equated equivalents between the Michael substrates **5a** and **3** and malononitrile (**2**) ($[BMN]_0/[DD]_0/[MN]_0 = 3:3:3$). A possible explanation for this observation can be found in the protonation step of the anionic species following nucleophilic attack of the deprotonated dimedone on benzylidenemalononitrile. Adding malononitrile to the ethanolic solution offers another proton source able to quench the negative charge and therefore prevent the intermediate from dissociating again in the Michael substrates. The formation of side product could not be observed in the Michael system with added malononitrile (Figure S5A).

Taking all these effects into account, it became impossible to postulate a rate law that fits to the obtained experimental data of the multicomponent reaction. Since all observed effects change with the respective concentrations and all concentrations change over reaction time, the rate law will be highly complex. In summary, the domino reaction is far from behaving like two independent, consecutive reactions. We also verified this complexity by comparing the experimental results of the one-pot multicomponent synthesis with modeled data for a consecutive first order–second order reaction kinetics under the assumption of two completely independent reactions (Section S4 and Figure S6 in the SI).

Implementation into Experimental Design Comparing One-Pot with Sequential Synthesis

After investigating the kinetics of the multicomponent domino reaction in detail, the question arose if this mechanistic information could be exploited to develop a more efficient continuous-flow synthesis than realized in the classical one-pot design for this specific reaction system. Therefore, a flow configuration was assembled that allows switching between one-pot and sequential designs in a straightforward manner. The sequential design, however, was not used to run one elementary reaction of the domino reaction after the other, as

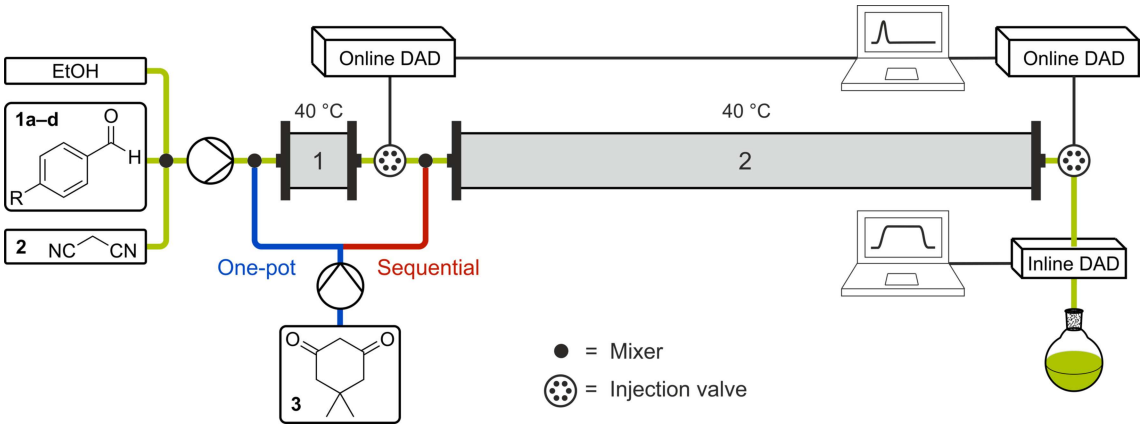

Figure 3. Experimental setup of the automated flow reactor for convenient switch between a classical one-pot design and a sequential design by moving the point at which dimedone solution is added. A short (5 mm) pre-reactor (1) was mounted in front of a longer (50 mm) main reactor (2) (dimensions of both are drawn to scale in the figure). Injection valves behind each reactor allow for online analysis by HPLC. Steady-state operation of the system was verified by an inline DAD.

classically done in flow chemistry applications. This classical sequential reaction design is even regarded as a hallmark of flow chemistry since the reaction mixture can be simply carried through individual units with different reaction parameters, in contrast to multistep batch experiments where reaction conditions must be adjusted for every single step.[28,39,40] Instead, a main reactor was employed together with a much smaller reactor preceding the main reactor. The purpose of the latter pre-reactor is to initiate the multicomponent reaction on the main reactor by providing a short introduction zone, in which the Knoevenagel reaction is allowed to proceed unhindered but which is not large enough to complete the reaction. The dimedone is added behind this pre-reactor, just before entering the main reactor, so that all three substrates are present on the main reactor and the reaction proceeds again in a multicomponent manner. For the experimental implementation, an additional pump as well as a second reactor and injection valve were assembled in the existing system (Figure 3). As main reactor, an aminopropylated silica monolith (4.6 mm inner diameter, 50 mm length) was applied; as pre-reactor, a same but shorter monolith (5 mm length) was mounted in front of it. The Knoevenagel substrate solutions were still mixed and pumped by the quaternary pump, however, the dimedone solution is now delivered by an extra binary pump. This straight design allows to move the point of dimedone addition within the flow system just by changing between the respective connecting capillary tubings (blue versus red in Figure 3). Injection valves were placed behind each reactor and were connected in series such that both valves injected to the same HPLC system.

Moreover, based on our insights gained from the multicomponent reaction kinetics, the equivalent ratio of malononitrile was increased from 1.0 to 1.2 (its starting concentration raised from $[MN]_0 = 10\ mmol\ l^{-1}$ to $12\ mmol\ l^{-1}$), because higher malononitrile concentrations not only improved the rate constants of the slow Michael addition step; in addition, the malononitrile prevents possible enrichment zones of the benzaldimine species (and associated side product formation) towards the reactor outlet. A little substrate scope of para-substituted aromatic aldehydes was applied (Scheme 1) to adjust the overall rate of the multicomponent reaction, taking into account that both elementary reactions rely on a nucleophilic attack in the mechanism. Functional groups characterized by an electron-releasing effect (methoxy and dimethylamino groups, **1 b** and **1 c**), which come along with bathochromic shifts in the UV-Vis spectra (Figure S7), lower the reaction rate. Functional groups causing a hypsochromic shift (trifluoromethyl, **1 d**) are considered as electron-withdrawing, which favors the nucleophilic attack on the aldehyde. The effect of substituents in the para-position of benzene derivatives on the reaction rates is described by the Hammett equation through the relationship between relative rates of product formation as a function of substituent constants known as σ_{para}-values, with negative values for the dimethylamino and methoxy substituents and a positive value for the trifluoromethyl substituent compared to the reference system benzaldehyde with $\sigma_{para} = 0$ (Table S2 and Figure S8).[41,42]

The multicomponent reactions of all four aldehydes (**1 a**–**d**) were run with the same experimental protocol (Experimental Section and SI). This also did not change when comparing the one-pot and sequential experimental designs. Under the assumption of the same maximum productivity, all substrate solutions were pumped with the same flow rates in the one-pot and in the sequential design so that the overall flow rates of both designs were matched. This means that in the sequential design the Knoevenagel substrate concentrations on the first (pre-)reactor are higher and reaction time is longer, since the dimedone stream is missing. In turn, the slow Michael addition step has less reactor space available than in the one-pot design, resulting in a shorter reaction time.

The data recorded for the substrate concentrations (Figure S9) and the areas of the product signals in the online HPLC chromatograms, shown in Figure 4, reveal a consistent trend: The change from the classical one-pot to the sequential

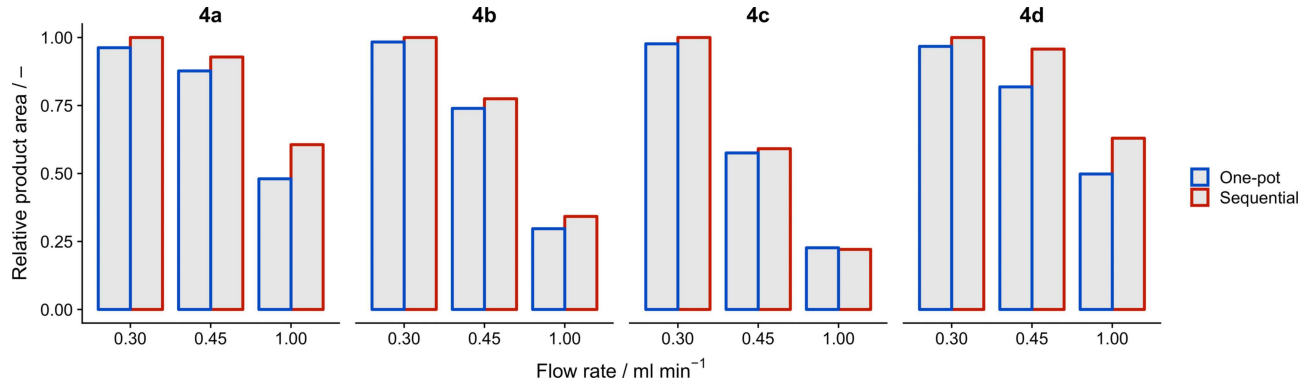

Figure 4. Relative product signal areas of tetrahydrochromene derivatives **4a–d** obtained by online HPLC (normalized to the largest area for each derivative), comparing the two different experimental designs (blue: one-pot design, red: sequential design; cf. Figure 3) for three system flow rates.

Table 1. Calculated turnover frequencies (TOFs) for the primary-amine catalyzed multicomponent reactions yielding the tetrahydrochromene derivatives **4a–d** at 40 °C in ethanol at an overall system flow rate of 1 ml min^{-1}. The two experimental designs are compared and the TOFs are summarized for both reactors separately as well as for the entire system as an average TOF. Besides the total TOFs of the catalyst, the turnovers are broken down into the respective substrate TOFs of the two different elementary reactions.

		TOF, reactor 1 (10^{-3} s^{-1})		TOF, reactor 2 (10^{-3} s^{-1})			TOF, both reactors (10^{-3} s^{-1})		
		Aldehyde	Total	Aldehyde	Dimedone	Total	Aldehyde	Dimedone	Total
4a	op[a]	1.34	1.78	0.63	0.48	1.11	0.70	0.48	1.17
	seq[b]	3.96	3.96	0.41	0.58	0.99	0.73	0.52	1.26
4b	op[a]	1.80	1.93	0.45	0.21	0.66	0.57	0.20	0.77
	seq[b]	3.08	3.08	0.37	0.23	0.60	0.62	0.21	0.83
4c	op[a]	0.50	0.48	0.15	0.01	0.17	0.18	0.01	0.19
	seq[b]	1.00	1.00	0.14	0.01	0.15	0.21	0.01	0.23
4d[c]	op[a]	2.02	2.59	0.41	0.45	0.86	0.56	0.46	1.02
	seq[b]	2.80	2.80	0.39	0.59	0.98	0.61	0.54	1.15

[a] One-pot design. [b] Sequential design. [c] Influenced by reverse Knoevenagel reaction.

experiment design not only leads to the expected higher conversions in the Knoevenagel reaction, but also yields higher multicomponent product concentrations of all tetrahydrochromene derivatives **4a–d** combined with higher dimedone conversions. It shows that the mechanistic and kinetic principles, which we have investigated in detail for the domino reaction with benzaldehyde (**1a**), can be transferred to a selection of aromatic aldehydes (**1b–d**) exhibiting strongly different overall reaction rates. The general trend reveals that the difference between both experiment designs increases with higher flow rates. It can be explained by the higher overall reaction rates under conditions with higher substrate concentrations at shorter reaction times.

To illustrate the cause for the better performance of the sequential design, the turnover frequencies of the active sites (TOFs) are provided in Table 1, comparing the two designs for the highest flow rate that was adjusted (1 ml min^{-1}). TOFs were calculated for the pre-reactor (reactor 1) and the main reactor (reactor 2) as well as for the entire system by averaging over both reactors. The data in Table 1 clearly show why the sequential experiment design outperforms the classical one-pot design. In the sequential design, the Knoevenagel reaction is so much boosted by the absence of dimedone on reactor 1 that the amount of produced intermediate (**5a–d**) becomes large enough to significantly overcompensate the missing reactor volume of reactor 1 for the Michael addition by a much higher reaction rate on reactor 2. The expected behavior of reaction rates adapted from the Hammett equation gets visible for the synthesis of the tetrahydrochromene derivatives **4a–4c**. For the trifluoromethyl substituted derivative **4d**, however, the catalyst unexpectedly shows lower TOFs than for the reference reaction yielding **4a**. This is explained by a significant reverse Knoevenagel reaction since the Knoevenagel product **5d** is very prone to hydrolysis. A Hammett plot of the Knoevenagel kinetics recorded behind reactor 1 showed the expected positive slope and is in good agreement with available literature (Figure S8).[43]

It is noteworthy that we have improved the efficiency of the catalyst just by changing a small detail in the experimental setup. Indeed, only an additional mixer is needed for the possible implementation in synthetic processes compared to the one-pot design. In this regard, enormous potential remains for additional optimization, since the lengths of the reactors (especially that of the pre-reactor used to initiate the multicomponent reaction) are expected to have an impact on the overall performance and were not optimized in this work. Furthermore, the classical reaction parameters such as the temperature, solvent, and concentrations remained unchanged, since an investigation of their interplay with an optimized experimental design is beyond (but may significantly extend) the scope of this work.

In general, the results illustrate that the TOFs of catalyzed reactions (and similarly, the conversion rates in uncatalyzed

reactions) not only depend on the chemistry itself, but are also significantly influenced by the technical implementation of the reaction, especially with increasing complexity of the chemical process. This is neither novel nor new,[44] but the focus typically is on the efficiency gain for a reaction process by trying out new reactivities (or new combinations of known reactivities). In contrast to these numerous studies, the deconvolution of the pertinent chemistry itself into elementary steps is strongly underrepresented, although tremendous optimization potential for chemical processes (and processings) rests behind this methodology and automation nowadays allows for time-efficient parameter-screening of chemical reactions. Moreover, this approach makes the optimization of chemical processes easier understandable und projectable for us humans, because the final experimental design is based on a causal chain of gathered findings on the relevant reactions.

Conclusions

We presented an empirical approach to improve the efficiency of a multicomponent reaction process by systematically studying the underlying reaction kinetics and mechanisms. An automated flow reactor was employed combining a high-performance catalytic microreactor with online HPLC analysis to tightly follow the reaction progress. This allows for time-efficient generation of data which – after processing and interpretation – deliver considerable information about the reaction system. In particular, we found for the multicomponent one-pot synthesis of tetrahydrochromene derivatives using benzaldehyde, malononitrile, and dimedone that the individual reaction steps of the domino Knoevenagel–Michael reaction interfere with each other. Due to the different role of the amine catalyst in both reactions, the substrates benzaldehyde and dimedone compete for the active sites of the heterogeneous catalyst. These findings were then implemented in a sequential experiment design (by adding a small pre-reactor in front of the main reactor), for which the catalyst showed significantly higher TOFs than in the one-pot control experiments with a set of four benzaldehyde substrates. The presented results can be easily transferred to homogenous catalysis or batch processes. Further, the importance of freely available active sites for the performance of the catalyst is highlighted – a key behind all catalytic processes. Ideally, only the mechanistically relevant substrate(s) interact with the catalytic centers and the technical execution of the reaction should be optimized in this regard.

Experimental Section

All compounds and solvents were purchased from standard commercial suppliers and were used without further purification. Additional details on the reaction setup, the monolithic catalyst support, as well as the synthesis and characterization (NMR, UV-Vis, HPLC, MS) of the intermediates **5a**–**d** and tetrahydrochromene derivatives **4a**–**d** can be found in the SI. For all shown reactions, tests were run to verify that reactions did not proceed in the absence of the catalyst. Moreover, catalyst poisoning did not play a role on the timescale of the measurements reported here.

Kinetics Studies: Kinetics studies on the single reaction steps as well as on the multicomponent reaction were carried out in ethanol (abs.) at 40 °C. Quasi-isothermal reaction conditions were achieved by pre-heating the reactant solutions and mounting the microreactor in a thermostatted column compartment. As microreactor served the commercially available and benchmarked silica-based monolith Chromolith® NH2 5-4.6 mm Guard Cartridge Kit obtained from Merck KGaA (Darmstadt, Germany). Bottle concentrations of the substrates benzaldehyde (**1a**), malononitrile (**2**), dimedone (**3**), and benzylidenemalononitrile (**5a**) were 30 mmol l^{-1}. Starting concentrations at the reactor inlet were adjusted automatically by the quaternary pump through the programmed mixing proportions. Five flow rates between 1.0–0.2 ml min^{-1} were adjusted for all combinations of concentrations, resulting in reaction times of ~4–21 s. An inline diode array detector (DAD) provided control over the steady-state status of the microreactor with high temporal resolution. For HPLC analysis, calibration of the commercially available UV-Vis active substances (**1**, **3**, **5a**) was performed prior to the kinetics studies. HPLC was run at 40 °C with water, deionized by a Milli-Q gradient purification system (Millipore, Bedford, MA), and ethanol under isocratic elution conditions (water/ethanol 67:33 v/v). As separation column served a Chromolith® HighResolution RP-18e 100-4.6 mm monolith from Merck. With an adjusted flow rate of 2 ml min^{-1}, an HPLC cycle was finished after 2.5 min so that the injection valve was programmed to inject a plug (1.3 μl) of the reaction solution every 150 s. Graphical visualization of the relevant programmed input parameters, the controlled process parameters, and the resulting HPLC chromatograms can be found for all executed experiments in the SI (Figures S10–S12).

Substrate Scope and Experimental Design Studies: To easily switch between one-pot and sequential experimental designs, the aldehydes **1a**–**d** (30 mmol l^{-1}) and malononitrile (**2**, 36 mmol l^{-1}) were still pumped by a quaternary pump, however, dimedone (**3**, 30 mmol l^{-1}) entered the system through a separate binary pump. The reactions were performed at 40 °C in ethanol (abs.) and substrate solutions were pre-heated in front of both reactors, which were mounted in thermostatted column compartments. For the pre-reactor (reactor 1), a commercially available and benchmarked aminopropylated monolith Chromolith® NH2 5-4.6 mm Guard Cartridge Kit (Merck) was adapted. For the main reactor (reactor 2), a similar but longer monolith was used (Chromolith® SpeedROD NH2 50-4.6 mm, Merck). For each benzaldehyde **1a**–**d**, both the one-pot and the sequential reaction design were investigated at three different system flow rates (1.00, 0.45, and 0.30 ml min^{-1}). HPLC cycles of 5 min were run with an isocratic period (2.25 min), a steep gradient (2.25 min) and a period for re-equilibration (0.5 min) at a flow rate of 2 ml min^{-1}. When both reactors reached steady-state operation, as verified by the inline DAD behind reactor 2, first the injection valve behind reactor 1 was switched to inject a plug (1.75 μl) of reaction solution onto the separation column. After the end of the HPLC cycle, the valve behind reactor 2, which was connected in series with the valve behind reactor 1, was switched with an injection volume of 1.3 μl. More details regarding HPLC analysis and the general workflow behind the substrate scope are summarized in the SI. There can also be found graphical visualization of the relevant programmed input parameters, the controlled process parameters, and the resulting HPLC chromatograms for all executed experiments (Figures S14–S21).

Acknowledgements

We thank Artur Svidrytski for providing the code for the numerical solution of the consecutive first order–second order reaction kinetics model (Figure S6).

Conflict of Interest

The authors declare no conflict of interest.

Keywords: heterogeneous catalysis · synthetic methods · multi-component reactions · domino reactions · kinetics

[1] R. Schlögl, *Angew. Chem. Int. Ed.* **2015**, *54*, 3465–3520; *Angew. Chem.* **2015**, *127*, 3531–3589.
[2] S. V. Ley, *Angew. Chem. Int. Ed.* **2018**, *57*, 5182–5183; *Angew. Chem.* **2018**, *130*, 5278–5279.
[3] N. Holmes, G. R. Akien, A. J. Blacker, R. L. Woodward, R. E. Meadows, R. A. Bourne, *React. Chem. Eng.* **2016**, *1*, 366–371.
[4] L. M. Baumgartner, C. W. Coley, B. J. Reizman, K. W. Gao, K. F. Jensen, *React. Chem. Eng.* **2018**, *3*, 301–311.
[5] J. M. Granda, L. Donina, V. Dragone, D.-L. Long, L. Cronin, *Nature* **2018**, *559*, 377–381.
[6] K. J. Kilpin, R. J. Whitby, *Chem. Cent. J.* **2015**, *9*, article no. 43.
[7] S. V. Ley, D. E. Fitzpatrick, R. J. Ingham, R. M. Myers, *Angew. Chem. Int. Ed.* **2015**, *54*, 3449–3464; *Angew. Chem.* **2015**, *127*, 3514–3530.
[8] C. P. Haas, T. Müllner, R. Kohns, D. Enke, U. Tallarek, *React. Chem. Eng.* **2017**, *2*, 498–511.
[9] R. Kohns, C. P. Haas, A. Höltzel, C. Splith, D. Enke, U. Tallarek, *React. Chem. Eng.* **2018**, *3*, 353–364.
[10] D. Enke, R. Gläser, U. Tallarek, *Chem. Ing. Tech.* **2016**, *88*, 1561–1585.
[11] D. Hlushkou, K. Hormann, A. Höltzel, S. Khirevich, A. Seidel-Morgenstern, U. Tallarek, *J. Chromatogr. A* **2013**, *1303*, 28–38.
[12] D. Stoeckel, C. Kübel, M. O. Loeh, B. M. Smarsly, U. Tallarek, *Langmuir* **2015**, *31*, 7391–7400.
[13] T. Müllner, K. K. Unger, U. Tallarek, *New J. Chem.* **2016**, *40*, 3993–4015.
[14] S.-J. Reich, A. Svidrytski, D. Hlushkou, D. Stoeckel, C. Kübel, A. Höltzel, U. Tallarek, *Ind. Eng. Chem. Res.* **2018**, *57*, 3031–3042.
[15] J. Yoshida, Y. Takahashi, A. Nagaki, *Chem. Commun.* **2013**, *49*, 9896–9904.
[16] J. S. Moore, K. F. Jensen, *Angew. Chem. Int. Ed.* **2014**, *53*, 470–473; *Angew. Chem.* **2014**, *126*, 480–483.
[17] I. M. Mándity, S. B. Ötvös, F. Fülöp, *ChemistryOpen* **2015**, *4*, 212–223.
[18] L. F. Tietze, A. Modi, *Med. Res. Rev.* **2000**, *20*, 304–322.
[19] C. Simon, T. Constantieux, J. Rodriguez, *Eur. J. Org. Chem.* **2004**, 4957–4980.
[20] H. Hagiwara, A. Numamae, K. Isobe, T. Hoshi, T. Suzuki, *Heterocycles* **2006**, *68*, 889–895.
[21] S. Balalaie, M. Bararjanian, A. M. Amani, B. Movassagh, *Synlett* **2006**, 263–266.
[22] M. M. Heravi, V. Zadsirjan, M. Dehghani, T. Ahmadi, *Tetrahedron* **2018**, *74*, 3391–3457.
[23] D. Grau, B. W. Grau, F. Hampel, S. B. Tsogoeva, *Chem. Eur. J.* **2018**, *24*, 6551–6556.
[24] I. R. Baxendale, *J. Chem. Technol. Biotechnol.* **2013**, *88*, 519–552.
[25] R. Munirathinam, J. Huskens, W. Verboom, *Adv. Synth. Catal.* **2015**, *357*, 1093–1123.
[26] B. Gutmann, D. Cantillo, C. O. Kappe, *Angew. Chem. Int. Ed.* **2015**, *54*, 6688–6728; *Angew. Chem.* **2015**, *127*, 6788–6832.
[27] A. Galarneau, A. Sachse, B. Said, C. H. Pelisson, P. Boscaro, N. Brun, L. Courtheoux, N. Olivi-Tran, B. Coasne, F. Fajula, *C. R. Chim.* **2016**, *19*, 231–247.
[28] S. Kobayashi, *Chem. Asian J.* **2016**, *11*, 425–436.
[29] M. B. Plutschack, B. Pieber, K. Gilmore, P. H. Seeberger, *Chem. Rev.* **2017**, *117*, 11796–11893.
[30] F. M. Akwi, P. Watts, *Chem. Commun.* **2018**, *54*, 13894–13928.
[31] S. Mozharov, A. Nordon, D. Littlejohn, C. Wiles, P. Watts, P. Dallin, J. M. Girkin, *J. Am. Chem. Soc.* **2011**, *133*, 3601–3608.
[32] T. Durand, C. Henry, D. Bolien, D. C. Harrowven, S. Bloodworth, X. Franck, R. J. Whitby, *React. Chem. Eng.* **2016**, *1*, 82–89.
[33] C. A. Hone, N. Holmes, G. R. Akien, R. A. Bourne, F. L. Muller, *React. Chem. Eng.* **2017**, *2*, 103–108.
[34] K. C. Aroh, K. F. Jensen, *React. Chem. Eng.* **2018**, *3*, 94–101.
[35] Y. Hayashi, *Chem. Sci.* **2016**, *7*, 866–880.
[36] R. Wirz, D. Ferri, A. Baiker, *Langmuir* **2006**, *22*, 3698–3706.
[37] S. L. Hruby, B. H. Shanks, *J. Catal.* **2009**, *263*, 181–188.
[38] M. J. Climent, A. Corma, S. Iborra, *RSC Adv.* **2012**, *2*, 16–58.
[39] D. Webb, T. F. Jamison, *Chem. Sci.* **2010**, *1*, 675–680.
[40] T. von Keutz, F. J. Strauss, D. Cantillo, C. O. Kappe, *Tetrahedron* **2018**, *74*, 3113–3117.
[41] L. P. Hammett, *J. Am. Chem. Soc.* **1937**, *59*, 96–103.
[42] C. Hansch, A. Leo, R. W. Taft, *Chem. Rev.* **1991**, *91*, 165–195.
[43] W. Li, S. N. Fedosov, T. Tan, X. Xu, Z. Guo, *ACS Catal.* **2014**, *4*, 3294–3300.
[44] P. S. Gromski, A. B. Henson, J. M. Granda, L. Cronin, *Nat. Rev. Chem.* **2019**, *3*, 119–128.